Biochemistry

 Volume 37, Number 47 November 24, 1998

Accelerated Publications

NO Reversibly Reduces the Water-Oxidizing Complex of Photosystem II through S_0 and S_{-1} to the State Characterized by the Mn(II)-Mn(III) Multiline EPR Signal†

Nikolaos Ioannidis, Josephine Sarrou, Gert Schansker, and Vasili Petrouleas*

Institute of Materials Science, NCSR "Democritos", 15310 Aghia Paraskevi Attikis, Athens, Greece

Received July 17, 1998; Revised Manuscript Received September 1, 1998

ABSTRACT: Incubation of photosystem II preparations with NO at −30 °C results in the slow formation of a unique state of the water-oxidizing complex (WOC), which was recently identified as a Mn(II)-Mn(III) dimer [Sarrou, J., Ioannidis, N., Deligiannakis, Y., and Petrouleas, V. (1998) *Biochemistry 37*, 3581−3587]. Evolution of the Mn(II)-Mn(III) EPR signal proceeds through one or more intermediates [Goussias, C., Ioannidis, N., and Petrouleas, V. (1997) *Biochemistry 36*, 9261−9266]. In an effort to identify these intermediates, we have examined the time course of the signal evolution in the presence and absence of methanol. An early step of the interaction of NO with the WOC is the reduction of S_1 to the S_0 state, characterized by the weak Mn-hyperfine structure recently reported for that state. At longer times S_0 is further reduced to a state which has the properties of the S_{-1} state, in that single-turnover illumination restores the S_0 signal. The Mn(II)-Mn(III) state forms after the S_{-1} state and is tentatively assigned to an (iso)S_{-2} state, although lower states or a modified S_{-1} state cannot be excluded at present. Following removal of NO 60−65% of the initial S_2 multiline signal size or the O_2-evolving activity can be restored. The data provide for the first time EPR information on a state lower than S_0. Furthermore, the low-temperature NO treatment provides a simple means for the selective population of the S_0, S_{-1} and the Mn(II)-Mn(III) states.

Water splitting by the oxygen-evolving complex (OEC[1]) of photosystem II (PSII) proceeds periodically during sequential absorption of photons. The OEC undergoes four one-electron oxidation-state transitions, $S_0−S_1$, ..., $S_3−S_4$. O_2 is released during the $S_4−S_0$ transition. After prolonged dark adaptation the complex is found in the S_1 state (see refs *1*−*5* for general reviews). The catalytic site of the OEC is a tetra-nuclear Mn cluster.

The study of the Mn cluster has benefited greatly from the application of EPR spectroscopy. Mn-centered EPR signals have now been detected for all three lower S states. The S_2 state is characterized by the extensively studied multiline signal at $g = 2$ (*6*) and the alternative signal at $g = 4.1$ (*7*, *8*); both are half-integer spin signals. The S_1 state is characterized by a broad integer spin EPR signal at $g = 4.8$ (*9*, *10*) and more recently by an alternative multiline signal at $g = 12$. The latter signal is detected in *Synechocys-*

* Corresponding author. Tel: +301 650-3344, -3349. Fax: +301 6519430. E-mail: vpetr@ims.ariadne-t.gr.

† This work was supported by the EC Grant ERBCHRXCT940524 and the PENED 1139 grant of the Greek General Secretariat of Research and Technology.

[1] Abbreviations: PSII, photosystem II; BBY membranes, thylakoid membrane fragments enriched in PSII; S states, S_0, ..., S_4 oxidation states of the water oxidizing complex; tyr Y_Z, tyr Y_D, the fast and slow tyrosine electron donors of PSII; Q_A, Q_B, the primary, secondary plastoquinone electron acceptors of PSII; cw EPR, continuous wave electron paramagnetic resonance; MES, 2-[*N*-morpholineethanesulfonic acid]; chl, chlorophyll; MeOH, methanol; OEC, oxygen-evolving complex; WOC, water oxidizing complex.

10.1021/bi981724e CCC: $15.00
Published on Web 11/01/1998

tis preparations and also, after removal of the 23 and 17 kDa extrinsic proteins, in spinach preparations (*11*). A half integer spin signal has been recently detected in the S_0 state produced either by chemical reduction (*12*) or after the 3d flash in a flash sequence (*13*, *14*). The presence of 0.5%−3% methanol is required for the observation of the weak hyperfine structure of the signal, but the signal is also observed as a broad derivative in the absence of methanol (*14*).

The observation of Mn-centered half-integer/integer/half-integer spin signals for the three states $S_0/S_1/S_2$ is consistent with the XANES data, indicating Mn oxidation during the one-electron S_0-S_1 and S_1-S_2 transitions (reviewed in ref *15*). A major unknown in these studies is, however, the oxidation-state composition of the Mn cluster in each of the above states. EXAFS experiments support a [2Mn(III)-2Mn(IV)] composition of the dark stable state S_1 (*15*−*17*), while theoretical simulations of the S_2 multiline EPR signal favor a [3Mn(III)-1Mn(IV)] (*18*) or a [1Mn(III)-3Mn(IV)] (*19*) composition. Other combinations are, however, possible and cannot be strictly excluded at present.

An EPR signal with prominent hyperfine structure has been detected in samples incubated with NO at −30 °C (*20*). The signal has been accurately simulated assuming an antiferromagnetically coupled Mn(II)-Mn(III) dimer (no detectable contributions from NO) (*21*). The S state assignment has not been made yet, but on the basis of its redox composition, the signal was tentatively assigned to a state lower than S_1, possibly lower than S_0, too (*21*). The position of this new state on a redox scale in comparison with the known S states is, however, a very important question, and to this end we have examined the intermediates of the signal formation. A study of the time course of the signal evolution in the presence and absence of methanol has revealed that the intermediates of the signal formation are the states S_0 and S_{-1}. Furthermore, it is shown that the conversion to the Mn(II)-Mn(III) state can be reversed by a number of illumination cycles and after removal of NO the WOC is active in oxygen evolution.

MATERIALS AND METHODS

PSII-enriched thylakoid membranes were isolated from market spinach by standard procedures (*22*, *23*) with some modifications. Samples for EPR measurements were suspended in 0.4 M sucrose, 15 mM NaCl, and 40 mM MES, pH 6.5, at 6−8 mg of chl/mL (4 mm EPR tubes). Illumination of the samples was performed with a 340 W projection lamp filtered through a solution of $CuSO_4$.

NO Treatment and the Effects of Methanol. The samples were bubbled in darkness at 0−4 °C with either pure NO or NO/N_2 mixtures for about 1 min and subsequently incubated at −30 °C for variable periods of time. The EPR NO peak at $g = 2$ served as an approximate measure of the free NO concentration. The free NO peak declined during the incubation at −30 °C. Although part of the observed decrease could be attributed to the consumption of NO by the interactions with the Mn cluster, the major part was attributed to nonspecific interactions or to dimerization of NO. The decline became increasingly pronounced in the presence of increasing concentrations of methanol in the range 0.5%−6% v/v, and this resulted in a severe delay in the reach of the final state, as described in the Results section. Addition of methanol after the NO treatment resulted in a decrease of the Mn(II)-Mn(III) signal size. This latter effect, which was more pronounced at 3% v/v methanol, is not examined further in the present investigation (but see the Discussion session).

EPR measurements were obtained with a Bruker ER-200D-SRC spectrometer interfaced to a personal computer and equipped with an Oxford ESR 900 cryostat, an Anritsu MF76A frequency counter, and a Bruker 035M NMR gaussmeter.

RESULTS

The original study of the interaction of NO with the S_1 state (*20*) indicated that the first step of this interaction was the loss of the ability to form the S_2 multiline signal by low-temperature illumination. This occurred much earlier than the evolution of the NO-induced multiline signal at −30 °C. At about 0.5−0.7 mM initial NO concentration the loss of the ability to form the S_2 multiline occurred with a halftime of 40−60 min while the multiline developed with a halftime of about 4−5 h. In the present study we have observed that the above characteristic times become significantly shorter, approximately halved, when the initial concentration of NO is approximately doubled by the use of pure NO. The assignment of the NO-induced signal to a Mn(II)-Mn(III) dimer (*21*) implied that NO acts effectively as a reductant of the S_1 state. The intermediate state with a $t_{1/2}$ of 40−60 min could accordingly be assigned to an early reduction event or to a modification of S_1 caused, for example, by the binding of NO. The recent discovery of an S_0 EPR signal (*12*−*14*) has offered a valuable experimental marker to test the two alternatives. As the S_0 signal is weak and the observation of its characteristic hyperfine structure requires the presence of methanol, the likely formation of the S_0 state could not have been detected in the earlier study, which was carried out in the absence of methanol. We have accordingly examined the intermediates of the NO treatment in the presence of methanol. Methanol was added either prior to or after the incubation with NO. Qualitatively similar results were obtained in the two cases.

The First Step of the Interaction of NO with S_1 Is Reduction to the S_0 State. Samples with 0.5%−3% methanol added were treated with NO for 1 min at 0 °C and subsequently incubated at −30 °C. Since methanol causes a rapid decrease of the free NO concentration (see Materials and Methods) pure NO was used in this experiment. EPR spectra were recorded at intervals of 15−30 min or longer. Figure 1 shows the progressive changes in the EPR spectrum of a sample pretreated with 3% methanol. The intense free NO peak at $g = 2$ was subtracted for clarity. Examination of the spectra shows the early evolution of a hyperfine structure with more intense lines on the low-field side and many weak lines extending over a broad magnetic field region. The hyperfine peaks reach a maximum in about 1 h and decline slowly at longer incubation times approaching the noise limit in about 8 h. On the other hand, no significant contributions from the Mn(II)-Mn(III) multiline signal develop either. This is mainly due to the relatively rapid decrease of the free NO level in the presence of methanol (see Materials and Methods). Addition of new NO results, indeed, in the

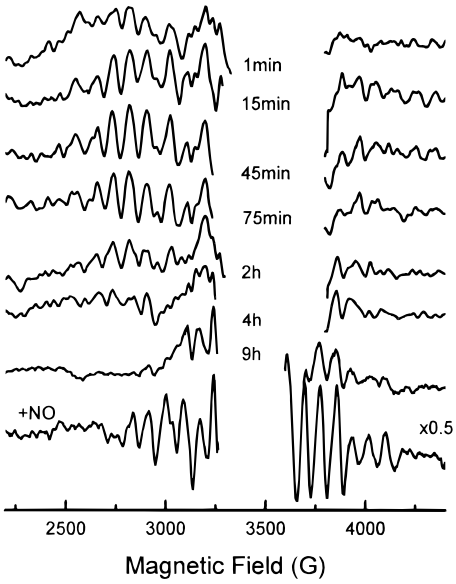

FIGURE 1: Progressive changes in the EPR spectrum of a sample incubated at −30 °C with pure NO in the presence of 3% MeOH. The formation and disappearance of the weak S_0 multiline signal are clearly shown. New NO was added at the end of the 9 h incubation period (see text for details), and this resulted in the relatively rapid (within 45 min) development of the Mn(II)-Mn(III) signal (lowest spectrum). The central part of the spectra which is distorted by the signal of free NO was removed for clarity: EPR conditions, $T = 6.5$ K; microwave frequency, 9.42 GHz; microwave power, 31 mW; modulation amplitude, 25 G_{pp}.

relatively rapid (within 30−60 min at −30 °C) evolution of the Mn(II)-Mn(III) signal, Figure 1.

In a different set of experiments, a number of samples were incubated with the same initial concentration of NO at −30 °C (typically 2:3 NO/N_2 ratios) for different periods of time, but shorter than those required for the formation of the Mn(II)-Mn(III) multiline (*20*, *21*). NO was subsequently removed, and methanol was added. Results qualitatively similar to those in Figure 1 were obtained (not shown).

Evolution of the new signal does not require incubation at −30 °C, as separate experiments have shown. We have restricted, however, the presentation to the −30 °C data in order to compare with the evolution of the Mn(II)-Mn(III) multiline. The new signal is more clearly presented in Figure 2 where it is compared with the S_2 and Mn(II)-Mn(III) multiline spectra. The signal shows strong similarities to the published S_0 spectra (*12*−*14*), and the similarity is further supported by the requirement of methanol for the observation of the hyperfine structure. The present signal has no discernible contribution of the broad ∼2400 G derivative-shaped signal (*14*). This may partially be due to the use of relatively high concentrations of methanol, 3% v/v, in the present study and to the baseline corrections (subtraction of the free NO peak), which may have removed broad signals underlying the weak hyperfine structure. The assignment of the present signal to the S_0 state is also supported by the fact that the evolution of the signal coincides with the loss of the ability of the complex to produce the S_2 multiline by single-turnover illumination. This follows from the earlier experiments in the absence of methanol (*20*) and also from experiments in the presence of methanol (not shown here but see Figure 4). Accordingly, this early step of the interaction of NO with the Mn complex is attributed to

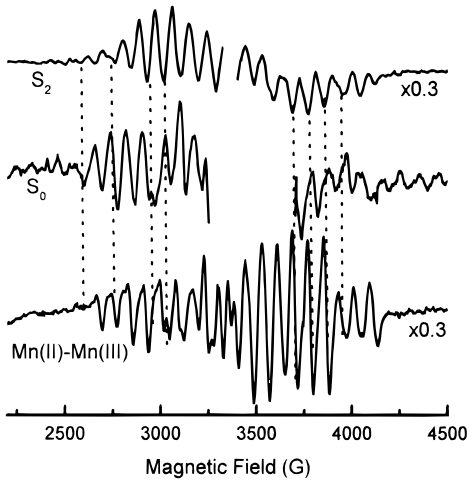

FIGURE 2: Comparison of the S_0 multiline with the spectra of the S_2 and the Mn(II)-Mn(III) states (note the different scaling factors in the spectra). The S_0 signal (average of four individual spectra) was produced during about 1 h of incubation with NO at −30 °C in the presence of 3% MeOH. EPR conditions are as in Figure 1.

reduction of S_1 to the S_0 state. The S_0 multiline signal is compared in Figure 2 with the Mn(II)-Mn(III) multiline. Strong differences are observed. A notable difference is in the width of the spectra. The overall width of the NO-induced multiline is 1600 G (2500−4100 G) (*21*), while the numerous lines of the S_0 signal extend over a spectral breadth of at least 2400 G (*12*−*14*). Certain low-field lines of the S_0 signal show an apparent coincidence with the low-field part of the Mn(II)-Mn(III) multiline, but the differences in the high-field part of the spectra are very pronounced. The larger breadth of the S_0 signal combined with a larger number of lines explains the significant difference in the intensity of the two signals. Another difference may be in the population of the two states, but this cannot be accurately determined at present.

A Subsequent Step Is the Reduction of S_0. The S_0 signal decreases on the hour time scale in Figure 1. The new EPR spectrum contains only minor contributions from the S_0 or the Mn(II)-Mn(III) multiline and therefore appears to represent a distinct state. We have examined whether this state results from the reduction of S_0. In a sample prepared in this state NO was removed and atrazine was added, so as to restrict light-induced oxidation to single-electron transfer. The spectra before and after illumination at 0 °C and subsequent dark adaptation for 20 min at 15 °C are shown in Figure 3, parts b and c, respectively, and are compared with the maximum S_0 signal, Figure 3a, obtained during the initial stages of incubation with NO. Clearly the spectrum following the illumination and dark adaptation—this latter step was included to allow for the decay of likely minor contributions from the S_2 state—is that of the S_0 state. Apparently, the new state that is produced concomitantly to the decrease of the S_0 signal shows the properties of the S_{-1} state. The spectrum in Figure 3c contains contributions from the Q_A-Fe^{2+} signal at $g = 1.82$ and 1.6. In untreated samples the dominant contribution from this state is at $g = 1.9$. It is interesting to note that the Q_A^--Fe^{2+} signals in Figure 3c do not decay during the 20 min dark adaptation at 15 °C. This is an additional manifestation of the fact that the state produced by the illumination is stable and therefore lower than the S_2.

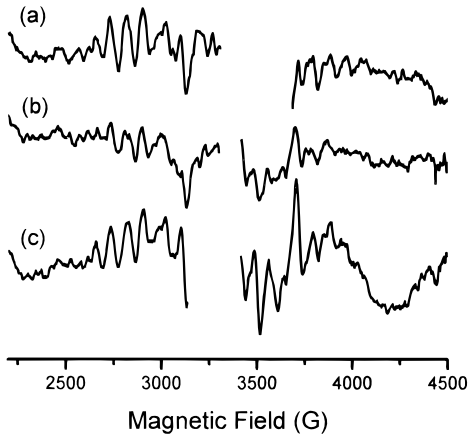

FIGURE 3: The loss of the S_0 signal during prolonged incubation with NO is due to reduction to the S_{-1} state. (a) The S_0 signal developed after 1 h of incubation with NO at −30 °C in the presence of 3% v/v MeOH. (b) Same sample after 9 h of incubation at −30 °C followed by removal of NO and addition of 0.1 mM atrazine. (c) Subsequent illumination at 0 °C followed by 15 min of dark adaptation at 15 °C. EPR conditions are as in Figure 1.

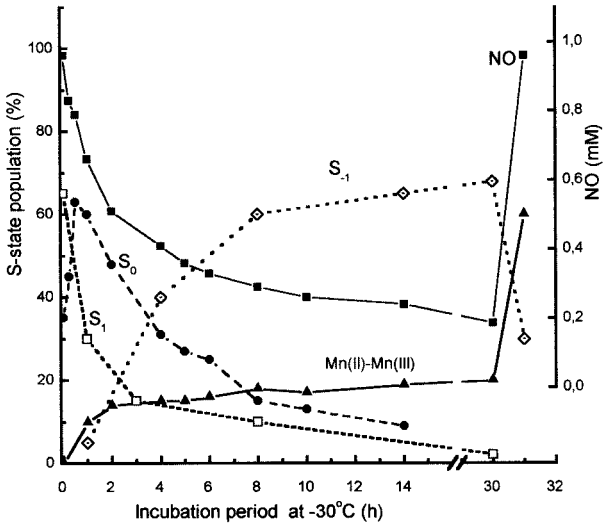

FIGURE 4: Gradual population/depopulation of the lower S states during the incubation at −30 °C with NO in the presence of 1.5% MeOH. The decline of the approximate concentration of NO is also shown. New NO was added after 30 h of incubation. See text for details on the estimation of the percentage population of the various states.

Qualitatively similar results were obtained in the absence of methanol. In this case the incubation with NO was interrupted at the point where a very small fraction of the Mn(II)-Mn(III) signal had developed. Following removal of NO, addition of methanol and atrazine, and illumination, spectra similar to those in Figure 3, parts b and c, were obtained (data not shown).

The S_{-1} state obtained in the above experiments probably contains contributions from adjacent states. Since illumination at 0 °C advances S_0 to the S_1 state, the S_0 multiline signal observed after the illumination is a measure of the centers in the S_{-1} state at the end of the incubation with NO.

The Mn(II)-Mn(III) State Forms after the Reduction to the S_{-1} State. The preceding experiments indicated that, regardless of the order of addition of methanol, the S_0 and S_{-1} states form prior to the formation of the Mn(II)-Mn(III) complex. The time course of the evolution of the S_0 and the Mn(II)-Mn(III) multiline signals has been studied with different methanol and NO concentrations. Qualitatively the results in all cases agree with the gradual population of the lower states as described above. With 3% methanol concentration the state obtained after prolonged incubation at −30 °C is primarily the S_{-1} state. With decreasing methanol concentrations (1.5%−0.5%), the terminal state contains increasing contributions from the Mn(II)-Mn(III) multiline. In the absence of methanol nearly the maximum Mn(II)-Mn(III) signal level is reached within 3−5 h when using pure NO. These differences are primarily attributed to the observed rapid decay of the free NO concentration in the presence of methanol (see Materials and Methods). Addition of new NO to a sample (3% methanol) following the decay of the S_0 signal and stabilization in the S_{-1} state, Figure 1, results in the relatively rapid evolution of a pronounced Mn(II)-Mn(III) multiline.

Figure 4 summarizes the evolution of the S_0 and the Mn(II)-Mn(III) signals in parallel with the observed decay of the free NO concentration in a sample pretreated with 1.5% methanol. The 0 of the time scale is set at the beginning of the incubation at −30 °C. The initial S_0 level is due to the preceding 1−2 min treatment with NO at 0−4 °C and to some pre-existing population of this state. Figure 4 shows in addition the approximate evolution of the population of the S_1 and S_{-1} states. To obtain the latter percentages a number of similar samples were incubated with NO for variable periods of time. NO was subsequently removed, atrazine was added, and the samples were illuminated at 0 °C and frozen. The spectra comprised generally a mixture of the S_2 and S_0 multiline signals, which could be discriminated by the fact that the S_2 multiline decays in less than one minute above 0 °C, while the S_0 signal remains stable over prolonged periods of time. The amounts of the S_2 and S_0 multiline signals were taken as a measure of the S_1 and S_{-1} state populations prior to the illumination. The population of the various states in Figure 4 is approximately normalized to the 100% level assuming that the size of the S_2 multiline signal, when compared to an untreated control, is an absolute measure of centers in the S_1 state. At the early incubation times (1 h) the levels of the S_{-1} and Mn(II)-Mn(III) states are insignificant and the depopulation of the S_1 is attributed mainly to the population of the S_0 state. The population of the S_{-1} state is indirectly estimated by comparing the S_0 signal produced by illumination with the normalized maximum signal of the S_0 state. The Mn(II)-Mn(III) signal is normalized by assuming that at long incubation times the S_{-1} and the Mn(II)-Mn(III) are the main states occupied. The self-consistency of these estimates is in turn examined by a comparison of the integrated EPR signal intensity of the Mn(II)-Mn(III) signal with that of the S_2 state. Due to the inherent very low intensity of the S_0 signal and the fact that the Mn(II)-Mn(III) signal exists in equilibrium with an EPR silent conformation, these estimates cannot be accurate. The largest uncertainty exists in the population of the S_{-1} and the Mn(II)-Mn(III) states at long incubation times, particularly after the addition of new NO. The presence of an EPR silent intermediate between the S_{-1} and the Mn(II)-Mn(III) states cannot, accordingly, be excluded at present.

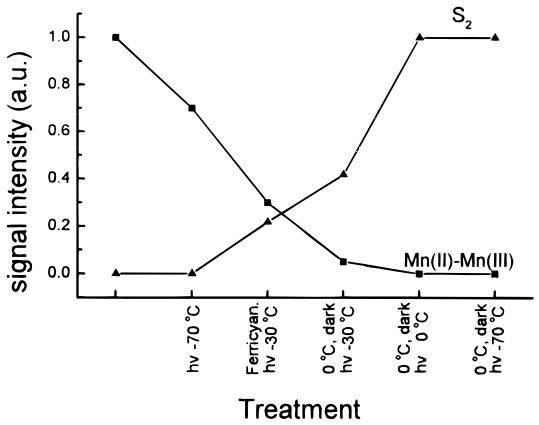

FIGURE 5: Light-induced decrease of the Mn(II)-Mn(III) signal and restoration of the S_2 multiline after a rather arbitrary sequence of illumination/dark-adaptation cycles. $K_3(FeCN)_6$ (0.2 mM) was added as an exogenous acceptor after the first illumination at −70 °C.

It is notable in Figure 4 that the level of NO between 8 and 30 h, although in excess of the PSII center concentration, is not sufficient for the evolution of the Mn(II)-Mn(III) signal. The requirement of significant levels of NO for the evolution of the latter signal cannot be easily understood without detailed knowledge of the interactions leading to the Mn(II)-Mn(III) signal formation. However, since NO acts as a reductant, it is possible that the addition of NO is required for lowering the ambient redox potential which may have been shifted upward by the accumulation of oxidation products of NO due to its interaction with the Mn cluster and other nonspecific interactions.

Reversibility of the Effects of NO. Restoration of the S_2 Multiline. The reduction of the cluster by NO leading to the Mn(II)-Mn(III) multiline signal proceeds through a number of steps, as it was illustrated above. An important question is whether the initial state can be restored by photochemical oxidation cycles. Perhaps the most stringent requirement spectroscopically is the restoration of the ability of the S_1 state to produce the S_2 multiline by low-temperature illumination. The Mn(II)-Mn(III) signal shows partial sensitivity to low-temperature illumination (−30 to −70 °C) (*20*). The efficiency of the low-temperature illumination appears to be higher (up to 70%) in samples incubated for 4−7 h with NO at −30 °C, compared to approximately 30% in samples incubated overnight or longer. Likely explanations are considered in the Discussion. The Mn(II)-Mn(III) signal is fully eliminated by a few cycles of low-temperature illumination followed by dark adaptation for several min at 4 °C, or more efficiently by continuous illumination at 0 °C. In the presence of ferricyanide as an exogenous electron acceptor a significant percentage of the S_2 multiline signal builds up. A subsequent dark adaptation brings the majority of the centers to the S_1 state, which shows low-temperature photochemistry identical to that of the untreated S_1 state. Figure 5 shows the evolution of the two signals during a rather arbitrary sequence of illumination and dark-adaptation cycles in the absence of methanol (similar results were obtained in the presence of methanol). Figure 6 compares the initial S_2 multiline signal with the signal obtained at the end of the illumination sequence. Approximately 60% of the initial S_2 multiline signal is restored. The only difference between the two signals is in the position of the acceptor side Q_A-Fe^{2+} signal, which following the NO treatment and removal of NO shifts to higher fields (see also Figure 3). This effect will be examined in a separate investigation.

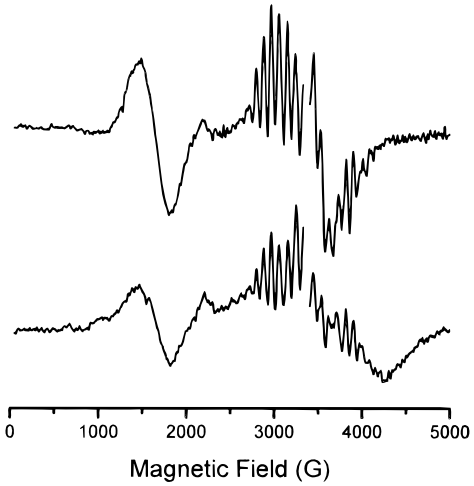

FIGURE 6: Comparison of the S_2 multiline recovered at the end of the illumination sequence of Figure 5 (lower), with the same signal in an untreated control sample (upper). EPR conditions are as in Figure 1.

O_2-Evolving Activity. Quantitatively similar results were obtained with the O_2-evolving activity. EPR samples were treated with NO so as to develop the maximum Mn(II)-Mn(III) signal. NO was subsequently removed, and the samples were diluted by about 800-fold. Compared to untreated controls, 65% of the O_2-evolving activity was measured under continuous illumination. Typical values in the presence 0.5 mM $K_3Fe(CN)_6$ and 0.2 mM 2,5-dichloro-*p*-benzoquinone as exogenous acceptors are 420 and 270 μmol of O_2/mg of Chl/h for the untreated and NO-treated samples, respectively.

DISCUSSION

The data provide evidence of an unprecedented gradual reduction of the Mn cluster by NO, which can proceed even at −30 °C. Furthermore the data present a rather simple method of a controlled population of the S_0, S_{-1}, and Mn(II)-Mn(III) states.

Understanding the Initial Observations. On the basis of the well-known affinity of NO for metal centers (mainly iron centers), the intermediates of the interaction of NO with the S_1 state were initially assigned to different modes/sites of binding of NO to the Mn cluster, although the possibility of NO acting as a reductant was also considered (*20*). The present results help to clarify most of the observations made in the initial study (*20*). Accordingly, the early loss of the ability to advance to the S_2 state by low-temperature illumination is due to the reduction of the S_1 state to S_0 and subsequently to S_{-1}. The Mn(II)-Mn(III) state appears to form as a result of reduction or modification of the S_{-1} state. It was observed that this latter step, unlike the early interaction with the S_1 state, is strongly retarded in the presence of moderately high, 50 mM, NaCl concentrations (*20*). This could be attributed to the attack by NO of two different sites, a chloride-insensitive step (early step) and a chloride-sensitive step (final step). A simpler explanation is, however, the following. It has been noted that the Mn(II)-Mn(III) signal exists in temperature equilibrium with an

EPR silent conformation (*20*, *21*). It is possible that high chloride concentrations favor the EPR silent conformation. In support of this, addition, in a preliminary experiment, of excess chloride (50 mM final) after creation of the Mn(II)-Mn(III) signal and removal of NO resulted in a decrease of the signal size by more than 60%. This effect is similar to the effect of methanol mentioned in the Materials and Methods section (see also ref *21*). Addition of 1.5% v/v methanol after the formation of the Mn(II)-Mn(III) signal resulted in an approximately 25% decrease in the signal intensity. At present it is not clear whether these molecules exert their effects by binding to the Mn cluster or more globally by altering the protein conformation.

On the Assignment of the Mn(II)-Mn(III) to a Lower S State. The OEC during its normal catalytic function cycles through states S_0 to S_4. Although the redox composition of the Mn cluster in any of the S states has not been unambiguously determined yet, it is generally agreed that high valence Mn exists even in the S_0 state. Suggested redox configurations for this state range from [Mn(II), 3Mn(III)] to [Mn(III), 3Mn(IV)] (see ref *14* and references therein). Therefore a number of oxidation states lower than S_0 are possible before all Mn is reduced to Mn(II). The study of these states could potentially provide important information on the Mn assembly process, the coordination changes that may occur in the higher states, as well as independent information on the electronic configuration of the cluster, etc. The information about these states is rather limited (see ref *24* and references therein) and probably confused by the fact that, depending on the reductant used, different isoelectronic configurations can be trapped (*25*) and also the cluster becomes unstable following extensive reduction (*25*, *26*). On the basis of flash O_2 studies coupled with reductive treatments of the Mn with hydrazine, Messinger et al. (*24*) reported the population of a S_{-3} state with almost 50% yield and they even suggested the likely existence of a S_{-5} state. No EPR spectra from any of the lower states have been reported so far. In this respect the Mn(II)-Mn(III) signal is the first EPR signal from a state lower than S_0. The present results show that the Mn(II)-Mn(III) state forms after the S_{-1} state. The most likely assignment would be, accordingly, to a state lower than S_{-1}, although a modified S_{-1} state cannot be excluded. A tentative assignment, which would have the smallest number of assumptions, is to an (iso)S_{-2} state composed of two non- (or very weakly) interacting dimers: a Mn(II)-Mn(III) dimer with a paramagnetic ground state and a second dimer (e.g., Mn(III)-Mn(III) or Mn(II)-Mn(IV) or even Mn(II)-Mn(II)) with a diamagnetic ground state. These possibilities will be hopefully clarified in future investigations.

Light Sensitivity and Activity Tests. The recovery of the S_2 multiline and the oxygen-evolving activity of the sample indicates that the reduction of the WOC by NO can be reversed in the largest fraction (60%−65%) of the centers. The inactive fraction of centers is probably due to some Mn loss during the reduction and after removal of NO and the subsequent aerobic handling of the samples (addition of exogenous acceptors and/or dilution for the O_2 measurements). The limited low-temperature light sensitivity of the Mn(II)-Mn(III) signal could be due to the requirement of a structural rearrangement of the cluster before advancement to a higher state can be possible. Slight structural rearrangements would not necessarily be rate-limiting to the O_2 evolution measurements recorded under continuous illumination. It should be noted that formation of the nitroso-tyrosine adduct (*27*), which could act as a competitive low-temperature donor was very limited under the present experimental conditions (*20*).

In conclusion, the present data have advanced significantly our understanding of the mechanism of the NO effects on the Mn cluster. Accordingly, the S_0 and S_{-1} states are intermediates of a reductive process leading to the unique Mn(II)-Mn(III) signal evolution. The latter is tentatively assigned to an (iso)S_{-2} state.

ACKNOWLEDGMENT

We thank Dr. I. Deligiannakis and Dr. J. Hanley for useful discussions and Mr. P. Vasilopoulos for technical support.

REFERENCES

1. Rutherford, A. W. (1989) *Trends Biochem. Sci. 14*, 227−232.
2. Debus, R. J. (1992) *Biochim. Biophys. Acta 1102*, 269−352.
3. Diner, B. A., and Babcock, G. T. (1996) *Advances in Photosynthesis: Vol. 4 Oxygenic Photosynthesis: The Light Reactions* (Ort, R. D., and Yocum, C. F., Eds.) pp 213−247, Kluwer Academic Publishers, Dordrecht, The Netherlands.
4. Bricker, T. M., and Ghanotakis, D. F. (1996) *Advances in Photosynthesis: Vol. 4 Oxygenic Photosynthesis: The Light Reactions* (Ort, R. D., and Yocum, C. F., Eds.) pp 113−136, Kluwer Academic Publishers, Dordrecht, The Netherlands.
5. Britt, R. D. (1996) *Advances in Photosynthesis: Vol. 4 Oxygenic Photosynthesis: The Light Reactions* (Ort, R. D., and Yocum, C. F., Eds.) pp 137−164, Kluwer Academic Publishers, Dordrecht, The Netherlands.
6. Dismukes, G. C., and Siderer, Y. (1981) *Proc. Natl. Acad. Sci. U.S.A. 78*, 274−278.
7. Casey, J. L., and Sauer, K. (1984) *Biochim. Biophys. Acta 767*, 21−28.
8. Zimmermann, J. L., and Rutherford, A. W. (1984) *Biochim. Biophys. Acta 767*, 160−167.
9. Dexheimer, S. L., and Klein, M. P. (1992) *J. Am. Chem. Soc. 114*, 2821−2826.
10. Yamauchi, T., Mino, H., Matsukawa, T., Kawamori, A., and Ono, T. (1997) *Biochemistry 36*, 7520−7526.
11. Campbell, K. A., Gregor, W., Pham, D. P., Peloquin, J. M., Debus, R. J., and Britt, R. D. (1998) *Biochemistry 37*, 5039−5045.
12. Messinger, J., Nugent, J. H. A., and Evans, M. C. W (1997) *Biochemistry 36*, 11055−11060.
13. Åhrling, K. A., Peterson, S., and Styring, S. (1997) *Biochemistry 36*, 13148−13152.
14. Messinger, J., Robblee, J. H., Wa On Yu, Sauer, K., Yachandra, V. K., and Klein, M. P. (1997) *J. Am. Chem. Soc. 119*, 11349−11350.
15. Yachandra, V. K., Sauer, K., and Klein, M. P. (1996) *Chem. Rev. 96*, 2927−2950.
16. Riggs, P. J., Mei, R., Yocum, C. F., and Penner-Hahn, J. E. (1992) *J. Am. Chem. Soc. 114*, 10650−10651.
17. Ono, T. A., Noguchi, T., Inoue, Y., Kusunoki, M., Matsushiata, T., and Oyanagi, H. (1992) *Science 258*, 1335−1337.
18. Zheng, M., and Dismukes, G. C. (1996) *Inorg. Chem. 35*, 3307−3319.
19. Hasegawa, K., Kusunoki, M., Inoue, Y., and Ono, T. A. (1998) *Biochemistry 37*, 9457−9465.
20. Goussias, C., Ioannidis, N., and Petrouleas, V. (1997) *Biochemistry 36*, 9261−9266.
21. Sarrou, J., Ioannidis, N., Deligiannakis, Y., and Petrouleas, V. (1998) *Biochemistry 37*, 3581−3587.
22. Berthold, D. A., Babcock, G. T., and Yocum, C. F. (1981) *FEBS Lett. 134*, 231−234.

23. Ford, R. C., and Evans, M. C. W. (1983) *FEBS Lett. 160*, 159−164.
24. Messinger, J., Seaton, G., Wydrzynski. T., Wacker, U., and Renger, G. (1997) *Biochemistry 36*, 6862−6873.
25. Riggs-Gelasco, P. J., Mei, R., Yocum, C. F., and Penner-Hahn, J. E. (1996) *J. Am. Chem. Soc. 118*, 2387−2399.
26. Beck, W., and Brudvig, G. W. (1987) *Biochemistry 26*, 8285−8295.
27. Sanakis, Y., Goussias, C., Mason, R. P., and Petrouleas, V. (1997) *Biochemistry 36*, 1411−1417.

BI981724E